Journal of Magnetism and Magnetic Materials 427 (2017) 245–250

Contents lists available at ScienceDirect

Journal of Magnetism and Magnetic Materials

journal homepage: www.elsevier.com/locate/jmmm

Titania-coated manganite nanoparticles: Synthesis of the shell, characterization and MRI properties

Zdeněk Jirák[a], Jarmila Kuličková[a], Vít Herynek[b], Miroslav Maryško[a], Jakub Koktan[a,c], Ondřej Kaman[a,*]

[a] Institute of Physics, AS CR, Cukrovarnická 10, 162 00 Praha 6, Czech Republic
[b] Institute for Clinical and Experimental Medicine, Vídeňská 1958/9, 140 21 Praha 4, Czech Republic
[c] University of Chemistry and Technology, Prague, Technická 5, 166 28 Praha 6, Czech Republic

ARTICLE INFO

Keywords:
Magnetic nanoparticles
Core-shell nanoparticles
Titania coating
Perovskite manganite
Magnetic resonance imaging
Transverse relaxivity

ABSTRACT

Novel procedure for coating of oxide nanoparticles with titania, employing hydrolysis and polycondensation of titanium alkoxides under high-dilution conditions and cationic surfactants, is developed and applied to magnetic cores of perovskite manganite. Bare particles of the ferromagnetic $La_{0.65}Sr_{0.35}MnO_3$ phase, possessing high magnetization, $M_{10\ kOe}(4.5\ K) = 63.5\ emu\ g^{-1}$, and Curie temperature, $T_C = 355$ K, are synthesized by sol-gel procedure and subsequently coated with titania. Further, a comparative silica-coated product is prepared. In order to analyse the morphology, colloidal stability, and surface properties of these two types of coated particles, a detailed study by means of transmission electron microscopy, dynamic light scattering, zeta-potential measurements, and IR spectroscopy is carried out. The experiments on the titania-coated sample reveal a continuous though porous character of the TiO_2 shell, the nature of which is amorphous but can be transformed to anatase at higher temperatures. Finally, the relaxometric study at the magnetic field of 0.5 T, performed to quantity the transverse relaxivity and its temperature dependence, reveals important differences between the titania-coated and silica-coated nanoparticles.

1. Introduction

Recent interest in magnetic nanoparticles is motivated by their prospects for biomedical and environmental applications. They may serve as the external field controlled carriers of drugs and biomolecules, negative contrast agents in magnetic resonance imaging (MRI), suitably supplementing Gd complexes, heating agents in the AC magnetic field induced hyperthermia for treatment of cancerous tissues, etc. [1,2]. In the treatment of waste waters, magnetic nanoparticles can be functionalized for remediation of heavy metals and various pollutants [3] or combined with chelating groups for selective removal of radioactive metals [4,5], allowing a recuperation of active agents in an external magnetic field. All these applications require additional modification of as-grown magnetic nanoparticles, in particular the hydrophilic coating that ensures the colloidal stability, eliminates the toxicity or even provides biocompatibility, or serves as an anchor for attaching of functional moieties [6].

The most common and endurable coating is formed by silica shell, which typically results from a hydrolysis of alkoxysilanes (e.g. tetraethoxysilane) and polycondensation of silicic species. As an alternative, the present study describes a new procedure whereby nanoparticles of the $La_{1-x}Sr_xMnO_3$ perovskite phase have been successfully covered with a continuous shell of titania. The particularly attractive feature of titania coating is, along with biological inertness or even biocompatibility, its electronic structure that provides excellent photocatalytic properties and is at the root of several promising medical applications [7]. Specifically, titania nanostructures can facilitate the highly localized photodynamic therapy of cancer [8,9], and they could be utilized as sensitizers for the sonodynamic therapy of deeply localized tumors [7].

As regards the magnetic cores, the manganites of the $La_{1-x}Sr_xMnO_3$ type have been selected instead of the prevalent iron oxide particles since they show, in the ferromagnetic range of composition ($x \approx 0.2$–0.5), extraordinary high transverse relaxivities, which suggests they could be used as efficient contrast and labelling agents in MRI [10,11]. Moreover, their magnetic behaviour can be efficiently controlled, including the possibility to adjust the Curie temperature in the range of 305–365 K [12]. Such feature, unprecedented in iron oxides, appeared prospective for the self-regulated hyperthermia [13,14]. The discussion of their medical or biological applications should

* Corresponding author.
E-mail address: kamano@seznam.cz (O. Kaman).

http://dx.doi.org/10.1016/j.jmmm.2016.10.097
Received 26 June 2016; Received in revised form 15 October 2016; Accepted 18 October 2016
Available online 19 October 2016
0304-8853/

definitely consider that potential leaching of harmful metal ions from these cores might pose a higher risk compared to iron oxide nanoparticles. However, several studies indicated that the issue of possible toxicity was resolved by suitable coatings [10,15,16].

In the following parts, the traditional sol-gel procedure is employed to prepare well-defined nanoparticles of $La_{0.65}Sr_{0.35}MnO_3$ composition, for which the highest magnetization is expected [12]. The magnetic cores are encapsulated into amorphous titania by means of titanium butoxide and surfactant-assisted procedure under high-dilution conditions. Further, a silica-coated sample is prepared to study the differences between the two types of shells. The following comparative analysis is focused on the morphology of the core-shell particles, their surface properties, and magnetic behaviour. To evaluate possible application of the particles in MRI, measurements of transverse relaxivity are performed in magnetic field of 0.5 T, and temperature dependence of the relaxivity is analysed.

2. Experimental details

2.1. Synthesis of $La_{0.65}Sr_{0.35}MnO_3$ nanoparticles (LSMO)

Manganite cores of the composition $La_{0.65}Sr_{0.35}MnO_3$ were prepared by a sol-gel process, using citric acid and ethylene glycol as chelating and gelling agents. The sol-gel precursor was subjected to calcination at 400 °C for 4 h, and the final thermal treatment was performed at 800 °C for 3 h. Subsequent mechanical processing of the as-prepared product involved three cycles of rolling followed by mixer milling. For comprehensive details of the whole preparation procedure see Ref. [17].

2.2. Preparation of titania-coated manganite particles (LSMO@titania)

The LSMO nanoparticles (50 mg) were dispersed in 25 mL of 0.5 wt % aqueous solution of cetyltrimethylammonium bromide (CTAB) in a 250 mL round-bottom flask under application of ultrasound and mechanical agitation. After 4 h, the suspension was diluted by 150 mL of methanol. Then, a slow addition of titanium butoxide (100 μL) in 25 mL of absolute ethanol via a syringe pump began and continued for 12 h. After next 5 h of stirring, the particles were separated by centrifugation and washed several times with water and ethanol. Simple size fractionation was carried out by centrifugation of their aqueous suspension at 728 rcf for 10 min. The corresponding supernatant was separated as the final product (yield of 13% with respect to the weight content of manganite cores).

2.3. Experimental thermal treatment of titania-coated particles

The LSMO@titania sample, dried at 105 °C, was subjected to consecutive thermal treatments followed by XRD measurements. In the first set of experiments, the applied temperature was 300 °C, and the treatment lasted for 4, 12, and 24 h. In the second set of experiments, the heating was limited to 4 h, but the temperature was increased from 300 °C by 100 °C in each following experiment.

2.4. Preparation of silica-coated manganite particles (LSMO@silica)

The comparative silica-coated sample was prepared from the same batch of LSMO nanoparticles as the titania-coated product. The manganite cores were stabilized by citrate and then coated with silica in a mixture of ethanol, water, and ammonia according to the method detailed in the previous report [14]. The specific amounts of materials and composition of the reaction mixture employed for the present synthesis were: 300 mg manganite cores, 1.5 mL tetraethoxysilane, 675 mL ethanol, 180 mL water, and 45 mL ammonia. The final product was obtained as the supernatant after centrifugation at 728 rcf for 15 min (yield 34% with respect to the weight content of manganite cores).

2.5. Characterizations

The phase composition and crystal structure of the bare and titania-coated LSMO nanoparticles were studied by X-ray powder diffraction (XRD) with CuKα line (Bruker D8 diffractometer). The diffraction patterns recorded were analysed by means of the Rietveld method (program FULLPROF), and the crystal structure data employed for the refinement were obtained from ICSD. In particular, the mean size of LSMO crystallites, d_{XRD}, was evaluated from the peak broadening. This determination used the Thompson-Cox-Hastings pseudo-Voigt profile to separate the strain and size contributions, whereas the instrumental profile was determined on the basis of a strain-free tungsten powder with the crystallite size of 9.4 μm.

The size and morphology of the coated products were analysed by transmission electron microscopy (TEM, Philips CM 120). The colloidal stability and the hydrodynamic size of coated nanoparticles were probed by measurements of the dynamic light scattering (DLS) in pure water (Malvern Zetasizer Nano S). Complementary measurements of the zeta potential were performed by laser Doppler electrophoresis (Malvern Zetasizer Nano S), using a series of aqueous suspensions whose pH was adjusted by dilute HCl or NaOH solutions. The IR spectra were measured in KBr pellets after drying at 105 °C for 2 h (FTIR Nicolet Nexus spectrometer).

Magnetic properties of the bare and coated products were measured on well-compacted samples by SQUID magnetometry (Quantum Design MPMS XL). The ZFC-FC (zero-field-cooled and field-cooled) measurements were carried out at the magnetic field intensity H = 20 Oe, and the inflection point of the FC susceptibility was employed to estimate the Curie temperature.

2.6. Relaxometric measurements

Before the relaxometric measurements, the concentration of water suspensions of LSMO@titania and LSMO@silica nanoparticles was accurately determined through the analysis of manganese by atomic absorption spectroscopy (AAS) with flame atomization. The standard addition method was applied to suppress any matrix effects, and the whole analysis including the mineralization of samples was carried out in triplicates (for the mineralization procedure see Ref. [17]). The concentration of the suspensions was adjusted to c(Mn) = 0.1 mmol L^{-1} for the relaxometry. The transverse relaxation times were measured at the magnetic field B_0 = 0.5 T (Bruker Minispec relaxometer) as a function of temperature, that was controlled by an external water bath and probed directly in the suspension. A modified CPMG multi-echo sequence was employed, and the parameters are specified in Ref. [11].

3. Results and discussion

3.1. Synthesis, structure and surface properties

XRD analysis of the LSMO sample evidenced that manganite nanoparticles were prepared as a single-phase product with perovskite structure of the $R\bar{3}c$ symmetry. The Rietveld refinement of the manganite structure, using the LSMO diffraction pattern shown in Fig. 1a, provided lattice parameters a = 5.4874(8) Å and c = 13.3955(40) Å, and the mean size of crystallites d_{XRD} = 25 nm. The corresponding cell volume per formula unit, V/Z = 58.195(21) $Å^3$, is practically identical to the value 58.173(2) $Å^3$ reported for a bulk sample of the same composition sintered at 1050 °C under oxygen flow [12].

The diffraction analysis of the LSMO@titania product was undertaken in order to determine the form of TiO_2 phase. However, no other

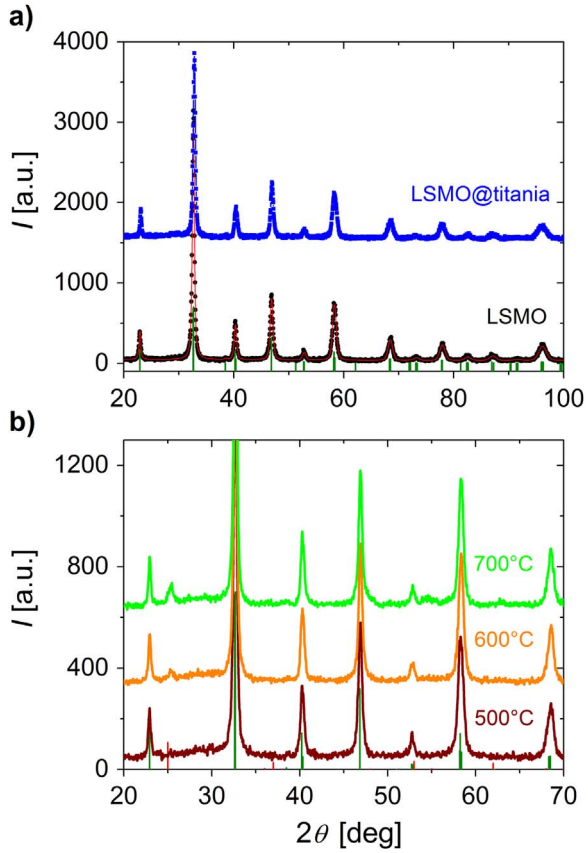

Fig. 1. XRD patterns: (a) bare and titania-coated $La_{0.65}Sr_{0.35}MnO_3$ nanoparticles, (b) titania-coated particles after the thermal treatment at gradually increasing temperature. The green vertical bars indicate diffractions of the perovskite phase of the rhombohedral symmetry (the pattern is derived from the structure with PDF number 01–089–0649), whereas red bars show the diffraction lines of anatase (PDF number 01-084-1285).

crystalline phases than the perovskite manganite were revealed (see Fig. 1a), which implies that the titania shell was fully amorphous in the as-prepared LSMO@titania material. Neither heating the dry LSMO@titania sample at 300 °C for 24 h nor treatment at 500 °C for 4 h lead to observable diffractions that could be assigned to any of TiO_2 polymorphic forms. Only after annealing at 600 °C for 4 h, a presence of the anatase form appeared obvious in XRD patterns. The intensity of characteristic diffraction lines further increased after the treatment at 700 °C, while the perovskite phase was still preserved (see Fig. 1b).

As the aforementioned XRD results are considered, the transformation of amorphous titania to anatase occurred at relatively high temperatures compared to several reports dedicated to synthesis of nanostructured anatase. However, the present experiments were performed as calcination of dry sample in air, and no optimization of the conditions was employed. Actually, strong catalytic effect of water for the crystallization of anatase was evidenced by previous studies, e.g. the XRD study of thermally treated amorphous titania demonstrated an efficient crystallization of anatase under hydrothermal conditions, whilst less crystalline product was obtained in water vapour at the same temperature, and only very weak diffraction of anatase was observed after treatment in dry atmosphere [18]. Finally, the present titania coating was deposited onto manganite cores by means of a CTAB-assisted procedure, whereby more porous materials generally result, and the comparison of the crystallization of precursors with different porosity may not be straightforward.

The morphology of the titania-coated particles is illustrated by transmission electron micrographs in Fig. 2a, b. The product is formed by well-dispersed core-shell particles that consist of small clusters of manganite crystallites, coated with a continuous but rather coarse titania shell of varying thickness ≈15–35 nm. Only minor fraction of free titania is observed. The comparative sample LSMO@silica (see Fig. 2c) is characterized by smaller size of both the coated particles and their magnetic cores. In contrast to titania, the silica shell is much more uniform with the mean thickness of 23(2) nm, and its surface is smooth. The described differences between LSMO@titania and LSMO@silica are related to the distinct coating procedures that have to be applied. First of all, the kinetics of hydrolysis and polycondensation of respective alkoxides is incomparably faster in the titania case [19]. The high reactivity of titanium alkoxides complicates the preparation of titania-coated nanoparticles since the heterogeneous nucleation of titania is hard to control, and the deposition on the surface of other nanoparticles might fail, while pure titania precipitates are formed. Therefore, a dilute solution of titanium butoxide in an anhydrous solvent was added continuously to manganite nanoparticles for a prolonged period, which simulated high-dilution conditions as the precursor was instantly reacting. Further, the use of CTAB surfactant, that provides the bare cores with colloidal stability and enables the successful deposition of titania, is responsible for higher porosity of the resulting shell compared to a surfactant-free procedure employed for coating with silica [20,21].

The different size of LSMO@titania and LSMO@silica nanoparticles was further confirmed by DLS measurements in water, that evidenced the colloidal stability of the aqueous suspensions as well. The intensity distribution of the hydrodynamic size is depicted in Fig. 3a for both the samples. The titania-coated and silica-coated particles are characterized by z-average values d_Z = 216 nm and 144 nm, respectively, while the validity of the DLS measurements is supported by rather low polydispersity indexes *pdi* = 0.049 and 0.113.

Zeta-potential measurements presented in Fig. 3b revealed strong coulombic repulsion among coated nanoparticles in water suspensions of LSMO@titania and LSMO@silica. At neutral pH, the surface of coated particles is charged negatively, providing them with high colloidal stability. The dependence of the zeta potential of LSMO@titania on pH should be discussed on the basis of a surface ionization model where two possible protonation sites have to be considered, namely the bridging oxygen Ti_2O and terminal oxygen TiO. Their protonation occurs due to the dissociative adsorption of water, while bridging and terminal hydroxyl groups are formed. According to the detailed study of titania by Panagiotou *et al.* [22], major fraction of Ti_2O is protonated even at alkaline pH = 10 and it increases to 95% below the isoelectric point (*pI*). In contrast, the protonization of terminal oxygen is limited even at low pH, whereas these sites are nearly completely deprotonated above *pI*.

The isoelectric point of the studied sample LSMO@titania, *pI* = 4.3, was found to be higher than the one of the silica-coated product, *pI* = 3.1, which is in accordance with published data on comparative measurements of pure silica and pure titania nanoparticles [23]. In contrast to titania, the pH dependence of zeta-potential of LSMO@silica nanoparticles is predominantly determined by the acidobasic properties of silanol groups that form a constitutive part of the silica shell, the composition of which should be described by the formula $SiO_x(OH)_y$ if thermal treatment at higher temperature is not applied [24].

IR spectra of bare LSMO cores and titania-coated product are presented in Fig. 4. The bare sample shows an absorption band at 605 cm^{-1}, where the stretching mode within MnO_6 octahedra is manifested [25]. However, this mode is obscured in the spectrum of LSMO@titania by the broad band of amorphous titania at 595 cm^{-1}, that exhibits typical features of material prepared by sol-gel procedures [26].

3.2. Basic magnetic properties and transverse relaxivity in MRI

The hysteresis loops of all studied samples at low and room temperatures are shown in Fig. 5. The response of bare LSMO

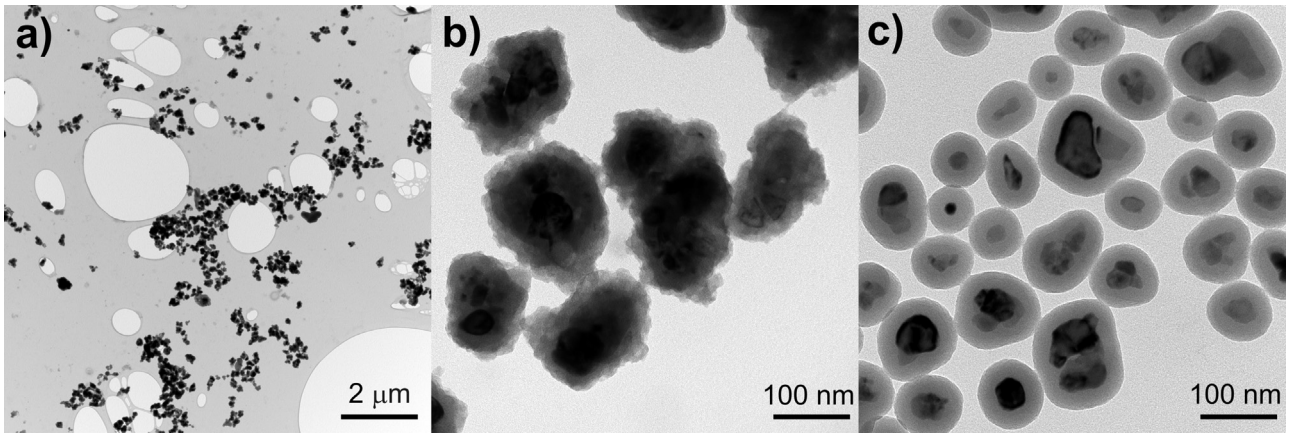

Fig. 2. TEM images: (a, b) titania-coated $La_{0.65}Sr_{0.35}MnO_3$ nanoparticles, (c) the same magnetic cores coated with silica shell.

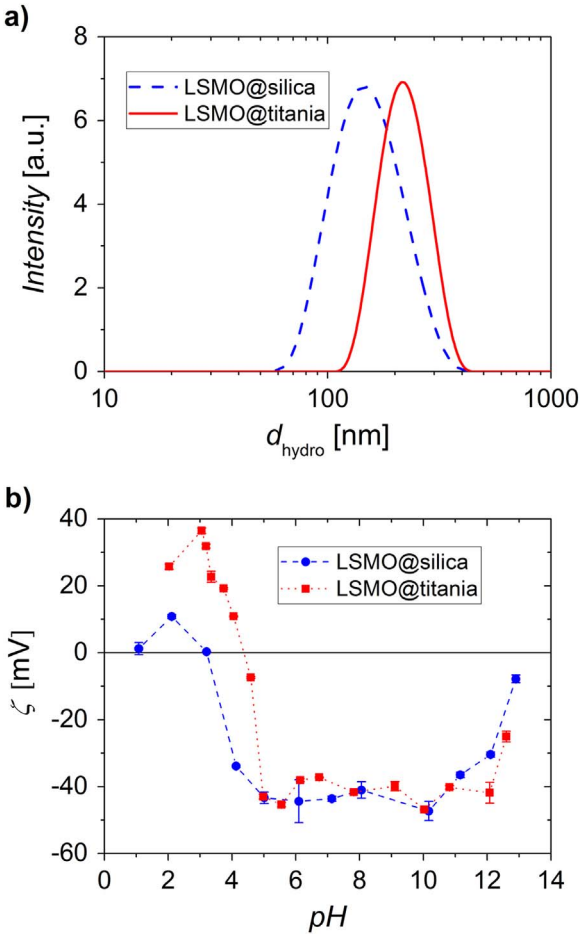

Fig. 3. Colloidal stability of titania-coated and silica-coated $La_{0.65}Sr_{0.35}MnO_3$ nanoparticles in water: (a) intensity distribution of hydrodynamic size d_{hydro}, (b) dependence of the zeta potential on pH.

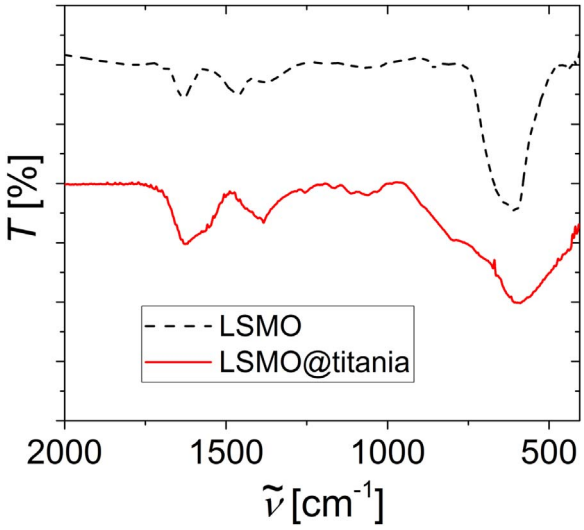

Fig. 4. IR spectra of titania-coated product and bare particles in KBr pellets. The spectra show the dependence of transmittance T on wavenumber $\tilde{\nu}$.

nanoparticles to an external field arose from the ferromagnetic arrangement of Mn spins, but the sample showed reduced magnetization (M(4.5 K) = 63.9 emu g^{-1} at H = 12.6 kOe) and Curie temperature (T_C = 355 K) compared to its bulk counterpart (M(4.5 K) = 89.5 emu g^{-1} at 12.6 kOe and T_C = 375 K according to [27]). The lower Curie temperature was already discussed as the effect of finite size of nanocrystals, that delimits the correlation length of the magnetic arrangement, whereas the decreased magnetization was explained in relation to the so-called magnetically dead layer, which is (in contrast to iron oxide and ferrite nanoparticles) an inherent structural phenomenon of manganite particles [12,28,29].

The dramatic drop of mass magnetization found for LSMO@titania and LSMO@silica nanoparticles, see Fig. 5, suggests that the amount of diamagnetic coatings makes a significant part of both the products. The ratio of the mass magnetization of a coated sample to the magnetization of bare LSMO particles at low temperature, w_M, should roughly correspond to the weight fraction of the $La_{0.65}Sr_{0.35}MnO_3$ phase provided that the size distribution of manganite crystallites within the coated and the bare samples are comparable. Thus, the lower weight fraction of titania compared to silica (1 - w_M = 0.46 and 0.71 for LSMO@titania and LSMO@silica, respectively) might be attributed to the aforementioned larger size of clusters of crystallites coated within a single titania shell compared to the size of magnetic cores in the silica-coated product. Nevertheless, the different densities of titania and silica shells, albeit unknown due to the possibly different porosity (the application of the CTAB surfactant for preparation of titania increases the porosity of the deposited material [20]), might contribute to the observed difference as well.

The dissimilar size of clusters of manganite crystallites in the coated products, LSMO@titania and LSMO@silica, was further reflected by the blocking behaviour of particles, that was probed by ZFC-FC studies (see Fig. 6a for the ZFC-FC susceptibilities). As observed on TEM, magnetic cores of LSMO@silica are formed either by small clusters of very few crystallites or even single manganite crystallites. These magnetic cores are coated by diamagnetic shell that suppresses dipolar interparticle interactions, and the blocking temperatures are conse-

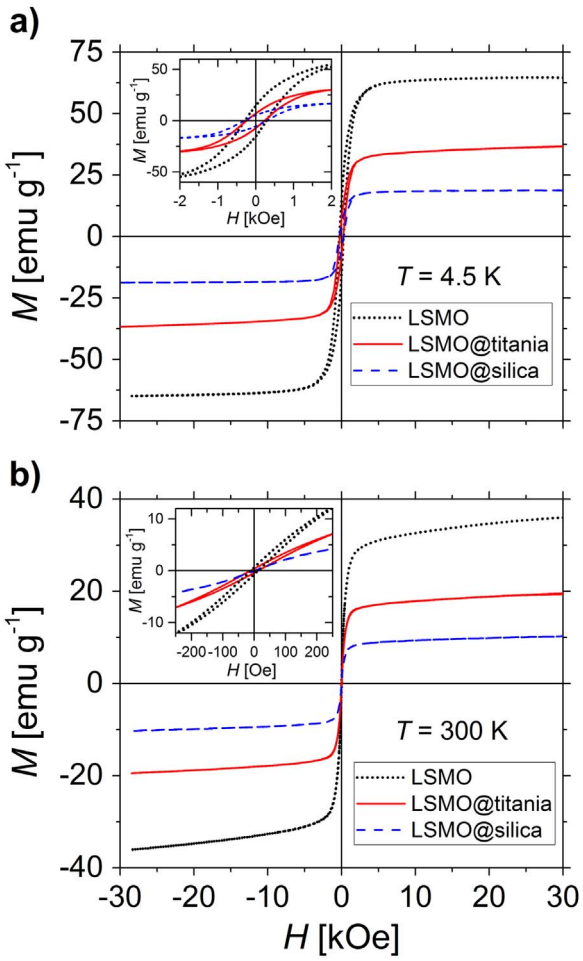

Fig. 5. Hysteresis loops of bare and coated $La_{0.65}Sr_{0.35}MnO_3$ nanoparticles at low (a) and room temperatures (b). The insets show low-field details of the loops.

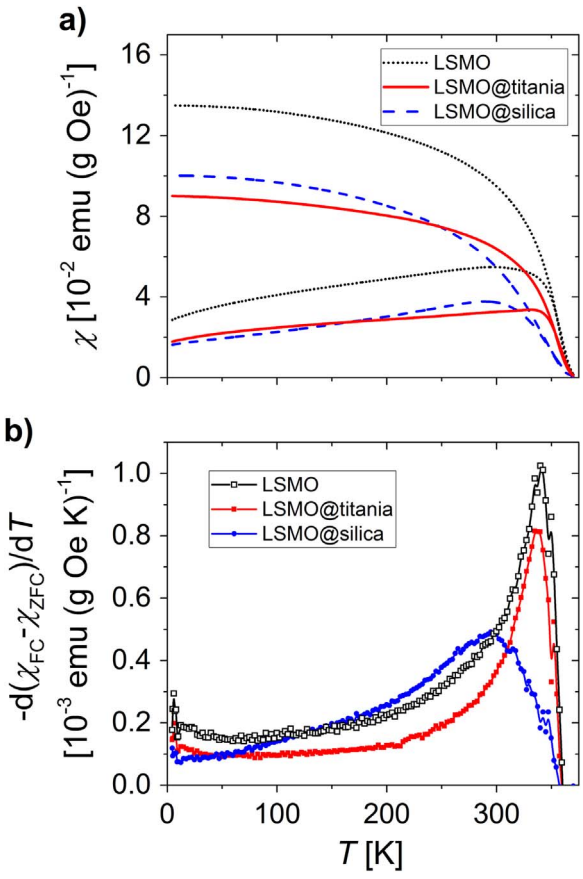

Fig. 6. ZFC-FC studies at the magnetic field intensity H = 20 Oe: (a) FC and ZFC susceptibilities, (b) the temperature derivative of the χ_{FC}-χ_{ZFC} susceptibility difference.

quently shifted to lower temperatures in comparison to the bare LSMO cores. This effect is particularly obvious from the derivative of the ZFC-FC susceptibility difference, depicted in Fig. 6b, that describes the blocking temperature distribution. The magnetic cores of LSMO@titania particles show blocking behaviour similar to the bare LSMO particles since the manganite crystallites involved, forming larger clusters, are still affected by strong dipolar interactions.

The measurements of transverse relaxivity at the magnetic field B_0 = 0.5 T, performed on the LSMO@titania and LSMO@silica products, are summarized in Fig. 7a. The value determined for the silica-coated nanoparticles at 20 °C was as high as r_2 = 460 s^{-1} $mmol(Mn)^{-1}$ L, which is in accordance with the value r_2 = 540 s^{-1} $mmol(Mn)^{-1}$ L reported for silica-coated $La_{0.65}Sr_{0.35}MnO_3$ nanoparticles with slightly larger d_{XRD} = 32 nm [11]. Lower r_2 values, albeit still high enough to exceed the contrast effect of commercial agents based on iron oxides [1], were found for the titania-coated product, specifically, r_2 = 280 s^{-1} $mmol(Mn)^{-1}$ L was determined at 20 °C.

As the temperature dependence of the relaxivity is concerned, the LSMO@silica particles are characterized by a substantial drop of the relaxivity from r_2 = 540 s^{-1} $mmol(Mn)^{-1}$ at 5 °C to 360 s^{-1} $mmol(Mn)^{-1}$ L at 35 °C, which correlates with observed decrease of their magnetization from M = 10.7 to 8.0 emu g^{-1}. In contrast, the LSMO@titania particles exhibited little variation of transverse relaxivity in the range 5–35 °C, with only a slight decrease from r_2 = 280 to 270 s^{-1} $mmol(Mn)^{-1}$ L. Let us note that this different behaviour cannot be ascribed to larger magnetic cores in the titania-coated product, since previous experiments on the silica-coated $La_{1-x}Sr_xMnO_3$ clusters showed a dependence of the r_2 values on the magnetic core size, but did not evidence any significant change in their temperature dependence (see the data in Fig. 7b) [30]. In this context, the temperature trend of transverse relaxivity observed in LSMO@titania is anomalous.

As a tentative explanation, we suggest that the fast exchange between molecules bound to the surface of particles and molecules of bulk water through diffusion and proton switching, that was facile in the suspension of LSMO@silica nanoparticles, is most likely hindered in the case of LSMO@titania. The titania shell is characterized by higher degree of immobilization of water protons due to its rough and porous character, which might prevent an efficient exchange. At the same time, water molecules diffusing well outside the large titania-coated particles experience only weak gradient of the magnetic field gradient, and their contribution to the transverse relaxation is not so significant. Thus, the observed temperature dependence of r_2 for LSMO@titania sample is strongly affected by the temperature dependence of the effective mobility of protons found in the vicinity of their cores. Their mobility increases with temperature, but the magnetic moment is decreasing at the same time, which might lead to a temperature invariant behaviour.

4. Conclusions

A novel procedure, developed for coating of metal oxide nanoparticles with titania, has been employed for the encapsulation of manganite nanoparticles of the $La_{0.65}Sr_{0.35}MnO_3$ composition. The method is based on the stabilization of particles by a cationic surfactant (cetyltrimethylammonium bromide), followed by a well-controlled hydrolysis and polycondensation of titanium butoxide under high-dilution conditions.

The titania-coated manganite nanoparticles are formed by somewhat larger clusters of crystallites than a comparable silica-coated

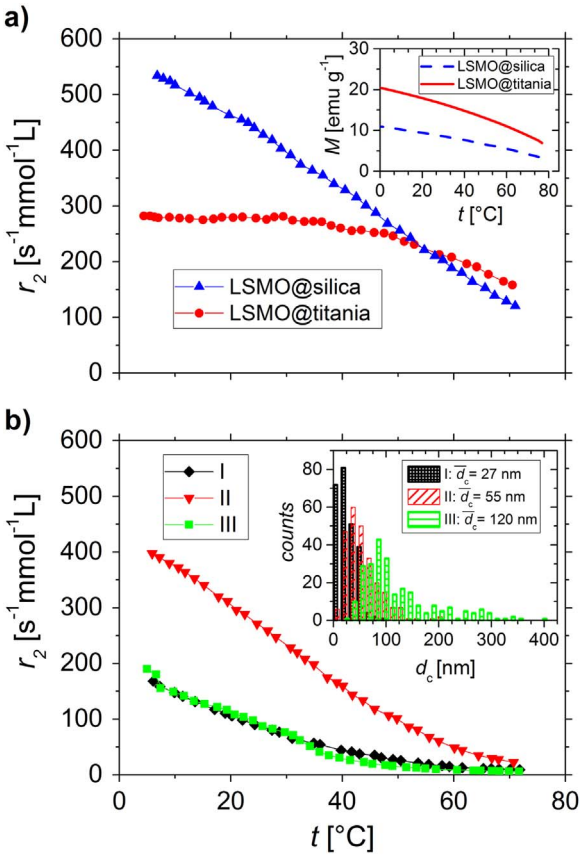

Fig. 7. Transverse relaxivity at B_0 = 0.5 T as a function of temperature: (a) dependences of r_2 observed for the present samples of titania-coated and silica-coated $La_{0.65}Sr_{0.35}MnO_3$ nanoparticles, supplemented by the temperature dependences of their magnetization (inset), (b) measurements reproduced from Ref. [30] showing dependences of r_2 for three different size fractions of silica-coated $La_{0.65}Sr_{0.35}MnO_3$ nanoparticles (T_C = 328 K, $d_{XRD} \approx$ 34 nm), the first one (I) was formed mostly by single-crystalline manganite cores, whereas the other two fractions (II and III) by clusters of crystallites (the size distributions of the diameter of whole magnetic core, d_c, evaluated from TEM data is shown in the inset together with the mean values $\bar{d}_c$).

product, but a reasonable hydrodynamic size is still achieved through a simple size fractionation. The coated particles form colloidally stable suspension in water, possess high magnetization, and provide strong negative contrast in MRI.

In contrast to silica-coated nanoparticles, that show a quasilinear decrease of transverse relaxivity, the relaxivity observed for the titania-coated manganite nanoparticles is nearly temperature independent except the region approaching Curie temperature. The different behaviours are discussed by considering the porosity and surface properties of these two coatings.

Acknowledgement

The study was financially supported by the Czech science foundation under the project 15-10088S. The MRI part of the research was supported through the project 16-04340S.

References

[1] S. Laurent, D. Forge, M. Port, A. Roch, C. Robic, L. Vander Elst, R.N. Muller, Magnetic iron oxide nanoparticles: synthesis, stabilization, vectorization, physicochemical characterizations, and biological applications, Chem. Rev. 108 (2008) 2064–2110.
[2] S. Mornet, S. Vasseur, F. Grasset, P. Veverka, G. Goglio, A. Demourgues, J. Portier, E. Pollert, E. Duguet, Magnetic nanoparticle design for medical applications, Prog. Solid State Chem. 34 (2006) 237–247.
[3] J. Liu, S.Z. Qiao, Q.H. Hu, G.Q. Lu, Magnetic nanocomposites with mesoporous structures: synthesis and applications, Small 7 (2011) 425–443.
[4] H. Zhang, R.G. McDowell, L.R. Martin, Y. Qiang, Selective extraction of heavy and light lanthanides from aqueous solution by advanced magnetic nanosorbents, ACS Appl. Mater. Interfaces 8 (2016) 9523–9531.
[5] M. Kaur, H. Zhang, L. Martin, T. Todd, Y. Qiang, Conjugates of magnetic nanoparticle-actinide specific chelator for radioactive waste separation, Environ. Sci. Technol. 47 (2013) 11942–11959.
[6] R.A. Sperling, W.J. Parak, Surface modification, functionalization and bioconjugation of colloidal inorganic nanoparticles, Philos. Trans. R. Soc. A-Math. Phys. Eng. Sci. 368 (2010) 1333–1383.
[7] F.U. Rehman, C. Zhao, H. Jiang, X. Wang, Biomedical applications of nano-titania in theranostics and photodynamic therapy, Biomater. Sci. 4 (2016) 40–54.
[8] R. Cai, K. Hashimoto, K. Itoh, Y. Kubota, A. Fujishima, Photokilling of malignant cells with ultrafine TiO_2 powder, Bull. Chem. Soc. Jpn. 64 (1991) 1268–1273.
[9] S.S. Lucky, N. Muhammad Idris, Z. Li, K. Huang, K.C. Soo, Y. Zhang, Titania coated upconversion nanoparticles for near-infrared light triggered photodynamic therapy, ACS Nano 9 (2015) 191–205.
[10] M. Kačenka, O. Kaman, J. Kotek, L. Falteisek, J. Černý, D. Jirák, V. Herynek, K. Zacharovová, Z. Berková, P. Jendelová, J. Kupčík, E. Pollert, P. Veverka, I. Lukeš, Dual imaging probes for magnetic resonance imaging and fluorescence microscopy based on perovskite manganite nanoparticles, J. Mater. Chem. 21 (2011) 157–164.
[11] P. Veverka, O. Kaman, M. Kačenka, V. Herynek, M. Veverka, E. Šantavá, I. Lukeš, Z. Jirák, Magnetic $La_{1-x}Sr_xMnO_3$ nanoparticles as contrast agents for MRI: the parameters affecting ^{1}H transverse relaxation, J. Nanopart. Res. 17 (2015) 33.
[12] P. Žvátora, M. Veverka, P. Veverka, K. Knížek, K. Závěta, E. Pollert, V. Král, G. Goglio, E. Duguet, O. Kaman, Influence of surface and finite size effects on the structural and magnetic properties of nanocrystalline lanthanum strontium perovskite manganites, J. Solid State Chem. 204 (2013) 373–379.
[13] E. Pollert, K. Knížek, M. Maryško, P. Kašpar, S. Vasseur, E. Duguet, New T_c-tuned magnetic nanoparticles for self-controlled hyperthermia, J. Magn. Magn. Mater. 316 (2007) 122–125.
[14] O. Kaman, P. Veverka, Z. Jirák, M. Maryško, K. Knížek, M. Veverka, P. Kašpar, M. Burian, V. Šepelák, E. Pollert, The magnetic and hyperthermia studies of bare and silica-coated $La_{0.75}Sr_{0.25}MnO_3$ nanoparticles, J. Nanopart. Res. 13 (2011) 1237–1252.
[15] M. Kačenka, O. Kaman, S. Kikerlová, B. Pavlů, Z. Jirák, D. Jirák, V. Herynek, J. Černý, F. Chaput, S. Laurent, I. Lukeš, Fluorescent magnetic nanoparticles for cell labeling: flux synthesis of manganite particles and novel functionalization of silica shell, J. Colloid Interface Sci. 447 (2015) 97–106.
[16] R. Haghniaz, K.R. Bhayani, R.D. Umrani, K.M. Paknikar, Dextran stabilized lanthanum strontium manganese oxide nanoparticles for magnetic resonance imaging, RSC Adv. 3 (2013) 18489–18497.
[17] O. Kaman, T. Dědourková, J. Koktan, J. Kuličková, M. Maryško, P. Veverka, R. Havelek, K. Královec, K. Turnovcová, P. Jendelová, A. Schröfel, L. Svoboda, Silica-coated manganite and Mn-based ferrite nanoparticles: a comparative study focused on cytotoxicity, J. Nanopart. Res. 18 (2016) 100.
[18] K. Yanagisawa, J. Ovenstone, Crystallization of anatase from amorphous titania using the hydrothermal technique: effects of starting material and temperature, J. Phys. Chem. B 103 (1999) 7781–7787.
[19] B.E. Yoldas, Hydrolysis of titanium alkoxide and effects of hydrolytic polycondensation parameters, J. Mater. Sci. 21 (1986) 1087–1092.
[20] R.I. Nooney, D. Thirunavukkarasu, Y.M. Chen, R. Josephs, A.E. Ostafin, Synthesis of nanoscale mesoporous silica spheres with controlled particle size, Chem. Mater. 14 (2002) 4721–4728.
[21] T. Peng, D. Zhao, K. Dai, W. Shi, K. Hirao, Synthesis of titanium dioxide nanoparticles with mesoporous anatase wall and high photocatalytic activity, J. Phys. Chem. B 109 (2005) 4947–4952.
[22] G.D. Panagiotou, T. Petsi, K. Bourikas, C.S. Garoufalis, A. Tsevis, N. Spanos, C. Kordulis, A. Lycourghiotis, Mapping the surface (hydr)oxo-groups of titanium oxide and its interface with an aqueous solution: the state of the art and a new approach, Adv. Colloid Interface Sci. 142 (2008) 20–42.
[23] D.H. Ryu, S.C. Kim, S.M. Koo, D.P. Kim, Deposition of titania nanoparticles on spherical silica, J. Sol.-Gel Sci. Technol. 26 (2003) 489–493.
[24] J.M. Kim, S.M. Chang, S.M. Kong, K.-S. Kim, J. Kim, W.-S. Kim, Control of hydroxyl group content in silica particle synthesized by the sol-precipitation process, Ceram. Int. 35 (2009) 1015–1019.
[25] K.B. Li, R.S. Cheng, S.G. Wang, Y.H. Zhang, Infrared transmittance spectra of the granular perovskite $La_{2/3}Ca_{1/3}MnO_3$, J. Phys. -Condes. Matter 10 (1998) 4315–4322.
[26] Z. Li, B. Hou, Y. Xu, D. Wu, Y. Sun, W. Hu, F. Deng, Comparative study of sol–gel-hydrothermal and sol–gel synthesis of titania–silica composite nanoparticles, J. Solid State Chem. 178 (2005) 1395–1405.
[27] M. Kačenka, O. Kaman, Z. Jirák, M. Maryško, P. Veverka, M. Veverka, S. Vratislav, The magnetic and neutron diffraction studies of $La_{1-x}Sr_xMnO_3$ nanoparticles prepared via molten salt synthesis, J. Solid State Chem. 221 (2015) 364–372.
[28] Z. Jirák, E. Hadová, O. Kaman, K. Knížek, M. Maryško, E. Pollert, M. Dlouhá, S. Vratislav, Ferromagnetism versus charge ordering in the $Pr_{0.5}Ca_{0.5}MnO_3$ and $La_{0.5}Ca_{0.5}MnO_3$ nanocrystals, Phys. Rev. B 81 (2010) 024403.
[29] Z. Jirák, M. Kačenka, O. Kaman, M. Maryško, N. Belozerova, S. Kichanov, D. Kozlenko, Role of surface on magnetic properties of $La_{1-x}Sr_xMnO_{3+\delta}$ nanocrystallites, IEEE Trans. Magn. 51 (2015) 1000204.
[30] T. Dědourková, O. Kaman, P. Veverka, J. Koktan, M. Veverka, J. Kuličková, Z. Jirák, V. Herynek, Clusters of magnetic nanoparticles as contrast agents for MRI: the effect of aggregation on transverse relaxivity, IEEE Trans. Magn. 51 (2015) 5300804.